Fission barriers for even-even superheavy nuclei

M. Kowal,[1,2,*] P. Jachimowicz,[2,3] and A. Sobiczewski[1,2]
[1]*Soltan Institute for Nuclear Studies, Hoża 69, PL-00-681 Warsaw, Poland*
[2]*GSI-Heimholtzzentrum für Schwerionenforschung (GSI), Planckstrasse 1, D-64291 Darmstadt, Germany*
[3]*Institute of Physics, University of Zielona Góra, Szafrana 4a, 65516 Zielona Góra, Poland*
(Received 10 May 2010; published 12 July 2010)

A quantitative model for the evaluation of the heights of static fission barriers is formulated within the framework of the macroscopic-microscopic approach. In order to describe the main properties (at the ground state and at the saddle point) of superheavy nuclei, a high-dimensional deformation space is used. In the present paper we systematically calculate fission barrier heights B_f for even-even heavy and superheavy nuclei in the range of proton numbers $92 \leqslant Z \leqslant 126$ and neutron numbers $134 \leqslant N \leqslant 192$. Comparisons with experimental data and different theoretical calculations are also shown. The dependence on B_f of fully incorporated, nonaxiality, and reflection-asymmetric degrees of freedom is discussed.

DOI: 10.1103/PhysRevC.82.014303 PACS number(s): 25.70.Jj, 25.70.Gh, 25.85.Ca, 27.90.+b

I. INTRODUCTION

There is no doubt that the considerable progress in the experimental synthesis of superheavy nuclei, which has been achieved by the DUBNA group [1–4] and recently partially confirmed at the GSI [5] and LBL laboratories [6], is stimulating for the theoretical evaluation of the possibility of producing new elements [7–18]. We believe that such an investigation might ultimately allow us to answer the basic question of whether or not there exists any limit for the mentioned process. The fundamental assumption which allows us to investigate the mechanism of the formation of superheavy compound nuclei is Bohr's hypothesis, which states that the synthesis of a compound system can be treated as a Markow type of process, a stochastic process without any memory effect. This implies that the exit channel is completely independent of the entrance channel as well as of the intermediate stage of the reaction that leads to the compound nucleus. The Bohr hypothesis can be justified mainly due to the different time scales of the particular stages. According to this hypothesis the total probability for the synthesis of new superheavy elements can be factorized into three independent ingredients:

$$P_{\mathrm{tot}} = P_{\mathrm{cap}} \times P_{\mathrm{for}} \times P_{\mathrm{dec}}$$

where P_{cap} stands for the probability of overcoming a Coulomb barrier, called the "capture process," P_{for} is the formation probability, where the nucleus, starting from the touching configuration, will finish up with a compound nuclear shape, and P_{dec} is the probability that the compound nucleus will survive without any subsequent decay. The knowledge of the shape of the fission barrier (i.e., its height and width), of the considered nucleus, is of greatest importance for the evaluation of the mentioned "survival probability," thereby used for the planning of any new synthesis experiment. In the spirit of the transition state theory (where full equilibration for all degrees of freedom inside of the barrier is assumed) the fission barrier depends only on two values of stationary points, one representing the ground-state minimum and the other the maximum of the energy. The aim of the paper is the calculation of the static fission barrier heights $B_f = E_{A(B)} - E_I$ (i.e., the difference between the energies at these two points for even-even superheavy nuclei). The standard notation for the first (A), or second (B) peak and for the global minimum, the ground state, (I) is used. The manuscript is organized as follows: first, we briefly describe details of the used macroscopic-microscopic method. Section II includes a description of all terms of the potential energy. Section IV presents the main ideas related to the shape parametrization of the nuclei at the ground state and at the saddle point. Section IV includes a discussion of the results and the influence on the fission barrier heights of various factors. Section V presents the summary and conclusions.

II. METHOD OF CALCULATION

In the past decades much effort has been undertaken to understand the physics of the fission process. It is, however, evident that its description, which is entirely based on a quantum-mechanical treatment, is out of scope due to the complexity of the fission process.

There also do not exist any "fundamental" models which would allow us to describe masses and fission barriers for heavy nuclei. All presently available models are in some sense "phenomenological's" (see, e.g., the interesting discussion about this subject in one of the latest publications of Möller *et al.* [19]). There are essentially two prescriptions which have proven quite successful: self-consistent mean-field studies based on some effective interaction or the macroscopic-microscopic method. Here we use the latter approach.

The total nuclear potential energy (E), which is a function of the shape, the proton number Z, and neutron number N, can be written as a sum of a macroscopic (E_{mac}) and a microscopic (E_{mic}) energy,

$$E(\mathrm{def}, Z, N) = E_{\mathrm{mic}}(\mathrm{def}, Z, N) + E_{\mathrm{mac}}(\mathrm{def}, Z, N). \quad (1)$$

All parameters that we use in the present paper are the same as those used in the calculation of masses and

*mkowal@fuw.edu.pl

equilibrium deformations of superheavy even-even nuclei [20], and odd-A and odd-odd [21] nuclei. We like to point out that our macroscopic-microscopic model is specially designed to describe the heaviest nuclei, and in the present paper it will be called the heavy-nuclei (HN) model (for heavy nuclei). One will notice that our approach does not contain any adjustable parameter, which could be fitted in the present study.

A. Macroscopic energy

For the macroscopic part, we used the Yukawa plus exponential model [22], as in many of our previous studies, with parameters specified in Ref. [20]. Deformation-dependent Coulomb and surface energies were integrated by using a 64-point Gaussian quadrature. No average pairing is used in the macroscopic energy. The influence of different macroscopic energies on various properties of superheavy nuclei has been discussed in Ref. [9].

B. Microscopic energy

The Strutinski shell correction [23], based on the deformed Woods-Saxon single-particle potential, is taken for the microscopic part:

$$E_{\rm mic}({\rm def}, Z, N) = \delta E_{\rm shell}({\rm def}, Z, N) + \delta E_{\rm pair}({\rm def}, Z, N), \tag{2}$$

where $\delta E_{\rm shell}$ and $\delta E_{\rm pair}$ are the shell and pairing corrections, respectively. The residual pairing interaction is treated fully microscopically by solving BCS equations. The strength of the pairing interaction is here assumed to be of the form:

$$AG_l = g_{0l} + g_{1l} I, \tag{3}$$

where A is the mass number and $I = (N - Z)/A$ is the relative neutron excess of a nucleus. The parameters g_{0l} and g_{1l} have been fitted to experimental odd-even mass differences as explained in Ref. [20].

The "universal" set of parameters of the potential given in [24] is chosen. The single-particle potential is diagonalized in the deformed-oscillator basis. The $n_p = 450$ lowest proton levels and $n_n = 550$ lowest neutron levels from the $N_{\rm max} = 19$ lowest shells of the oscillator are taken into account in the diagonalization procedure. We have determined the single particle spectra for every investigated nucleus. These calculations therefore do not include any scaling relation to the *central* nucleus. Standard values of $\hbar\omega_0 = 41/A^{1/3}$ MeV for the oscillator energy and $\gamma = 1.2\hbar\omega_0$ for the Strutinski smearing parameter γ, and a six-order correction polynomial are used in the calculation of the shell correction. Some advantages of the Strutinski smoothing method as compared to a Hartree-Fock type approach can be found by the reader (e.g., in the textbook by Hofmann [25]).

III. SHAPE PARAMETRIZATION

The essential point of our present investigation consists in the accuracy, and the kind and dimension of the deformation space which is used to describe very large variety of nuclear shapes with the vast multitude of degrees of freedom that a deformed nucleus can take all along the fission path. Of course, an ideal kind of parametrization should describe simultaneously not only equilibrium and saddle point shapes but also a reseparation of fragment shapes. As far as we are interested in the fission barriers for superheavy nuclei, a traditional parametrization of the shapes, which consists in the expansion of the nuclear radius in spherical harmonics [26], can be used

$$R(\vartheta, \varphi) = R_0\left(1 + \sum_{l=1}^{\infty}\sum_{m=-l}^{l} a_{lm} {\rm Y}_{lm}\right). \tag{4}$$

In the case of axially symmetric shapes ($m = 0$), it is convenient to use parameters β_l instead of a_{lm}. In the present paper we are limiting ourselves to consideration of shapes defined by

$$\begin{aligned} R(\vartheta, \varphi) = R_0[1 &+ \beta_2(\cos\gamma_2 {\rm Y}_{20} + \sin\gamma_2 {\rm Y}^{(+)}_{22}) \\ &+ \beta_4 {\rm Y}_{40} + a_{42}{\rm Y}^{(+)}_{42} + a_{44}{\rm Y}^{(+)}_{44} + \beta_3 {\rm Y}_{30} \\ &+ \beta_5 {\rm Y}_{50} + \beta_7 {\rm Y}_{70} + \beta_6 {\rm Y}_{60} + \beta_8 {\rm Y}_{80}]. \end{aligned} \tag{5}$$

The real functions ${\rm Y}^{(+)}_{lm}$ are defined as

$${\rm Y}^{(+)}_{lm} = \frac{1}{\sqrt{2}}[{\rm Y}_{lm} + (-1)^m {\rm Y}_{l-m}] \quad \text{for } m \neq 0. \tag{6}$$

For $l = 2, m = 0, 2$, we use conventional notation:

$$a_{20} = \beta_2 \cos\gamma_2, \quad a_{22} = \beta_2 \sin\gamma_2, \tag{7}$$

where γ_2 is the Bohr quadrupole nonaxiality parameter. The dependence of R_0 on the deformation parameters is determined by the volume-conservation condition. There is no physical principle which would forbid the nucleus from having a nonaxial ground-state shape. On the other hand, the calculations performed by Möller *et al.* [27] suggest that in the investigated vicinity of nuclei nonaxiality is practically negligible. Moreover, our preceding work [28] shows practically no effects of the nonaxial octupole deformations (tetrahedral symmetries) in the minimum on the potential energy. On the other hand, axially symmetrical competing minima in superheavy nuclei has been found recently [29]. For this reason, for all nuclei investigated by us, axially symmetric deformed shapes are assumed at the equilibrium point (ground state). The energy is minimized simultaneously in all axial degrees of freedom: β_2, β_3, β_4, β_5, β_6, β_7, β_8, using a multidimensional conjugate gradient method.

Beginning from the ground state, the energy of a nucleus increases along an effective one-dimensional trajectory in the multidimensional nuclear deformation space until it reaches the saddle point and then starts to decrease, creating the energy barrier along the fission path.

The potential energy is calculated in the following grid points:

$$\begin{aligned} \beta_2 \cos\gamma_2 &= 0(0.05)0.65, \\ \beta_2 \sin\gamma_2 &= 0(0.05)0.40, \\ \beta_4 &= -0.20(0.05)0.20. \end{aligned} \tag{8}$$

Numbers in the parentheses specify the step with which the calculation is done for a given variable. Then, the energy is

interpolated (by the standard SPLIN3 procedure of the IMSL library) to the five times denser grid in each variable. Thus, we finally have the values of the potential energy at a total of 110 946 grid points. In order to find the saddle point a two-step method is used. First, on such a three-dimensional grid (β_2, γ_2, β_4) the dynamic programming method is used [30], and, at the thus established saddle-point deformations, the energy is subsequently minimized with respect to the other degrees of freedom: $a_{42}, a_{44}, \beta_3, \beta_4, \beta_5, \beta_6, \beta_7, \beta_8$ (see the Appendix for more details). In previous calculations [31,32] the hexadecapole axial asymmetry parameter has usually been treated as a function of the quadrupole asymmetry angle γ_2. It should be noted that, in the present calculation, hexadecapole nonaxiality is not dependent on the quadrupole nonaxial deformation but it is taken it into account by using the a_{42}, a_{44} parameters.

IV. RESULTS

Let us begin our discussion with the description of numerical tests and error checks. One of the important numerical tools exploited by us here is the minimization procedure. It is used to find first the ground-state energy in a seven-dimensional space and, in a second step, through our saddle-point searching method, the saddle-point energy (in an eight-dimensional minimization). The not the multidimensional minimization method is a mixed blessing: from one point of view, it gives us the opportunity to find minima in the large deformation spaces (infeasible on the grid) but, on the other hand, it introduces the necessity to check whether or not the obtained minima are indeed the global ones. In order to gain some confidence in our results we used a number of checks. The standard checks within the minimization routine include the monitoring of energy gradients. In addition, we looked at the continuity of the resulting deformation parameters with respect to $\beta_2 \sin\gamma_2$ and $\beta_2 \cos\gamma_2$, and at their stability with respect to the choice of their starting values. The starting values of the deformation parameters were always taken differently from zero. It should also be realized that we cannot be absolutely certain that the minimization in the second step of our procedure does not lead to errors. The hope that the main deformation net ($\beta_2 \sin\gamma_2$, $\beta_2 \cos\gamma_2$, β_4) may be sufficient is based mainly on the fact that higher deformations are small and are weakly coupled to the main deformations in the studied nuclei. In addition, we have checked values of the energy at the obtained saddle points at the first stage in two cases: in a two-dimensional and a four-dimensional calculation. On the two-dimensional grid: ($\beta_2 \sin\gamma_2$, $\beta_2 \cos\gamma_2$) and on the four-dimensional grid with two variants: ($\beta_2 \sin\gamma_2$, $\beta_2 \cos\gamma_2$, β_4, a_{42}) and ($\beta_2 \sin\gamma_2$, $\beta_2 \cos\gamma_2$, β_4, a_{44}) of the saddle-point searching technique were used. One of the most important tests for the saddle-point searching method was the application of a completely different approach based on so-called "*imaginary water flow*" [19,33–36]. This conceptually simple and numerically efficient method in the five-dimensional case (i.e., $\beta_2 \sin\gamma_2$, $\beta_2 \cos\gamma_2$, β_4, a_{42}, a_{44}) has been used for some of the nuclei. We can report here that the results were practically identical. For several nuclei, we repeated the minimization for the whole map by choosing starting values randomly and found that the results agreed with the ones obtained previously.

A. Description of experimental fission barriers

We are now going to apply this formalism to examine the obtained fission barrier heights in actinides nuclei for which experimental data are available. However, one should keep in mind that the type of parametrization used, Eq. (4), describes distortions close to the spherical shape and for this reason it is rather suitable and properly defined for small deformations. Fortunately such a situation is encountered in the case of superheavy nuclei, where the barriers are rather short. This is, however, not at all the case for the actinides nuclei, with a very complicated topology of the potential-energy surface. Theoretical predictions that suggest the existence of a second, superdeformed (SD) and a third, hyperdeformed (HD) peak in some actinide nuclei [37–39] seem to be experimentally confirmed [40–43]. Owing to the complexity of the potential-energy surface in actinides, a better deformation space (including, e.g., "pear" nonaxial shapes related to spherical harmonics of the type Y_{32}, Y_{52}, Y_{72}) is probably still required for these nuclei. Additionally, for those nuclei calculations should be performed simultaneously in all degrees of freedom (without introducing any subdivision of relevant and irrelevant deformation subspaces), which will be handled in a forthcoming paper (in the context of such a global approach as presented here, it is difficult and still too time consuming from the numerical point of view). Therefore we start our discussion with a comparison of calculated first fission barriers in actinides (see Table I), occurring at $\beta_2 \approx (0.5 \div 0.6)$, which corresponds to the end of the fission barriers in superheavy nuclei.

Inner fission barriers $B_f = E_A - E_I$ (i.e., the difference between the first saddle-point E_A and the global ground-state energy E_I) are shown in Fig. 1. In the course of our work we face the problem of the zero-point vibration energy. The inclusion of such an energy correction usually boils

TABLE I. Comparison of the first fission barriers as in Fig. 1. All quantities are in MeV, except for numbers specifying the nucleus.

Z	N	A	LSD	FRLDM	HN	EXP
92	140	232	–	3.2	4.5	5.4
	142	234	4.4	3.8	5.1	5.9
	144	236	5.5	4.5	5.6	5.6
	146	238	6.7	5.1	5.9	6.0
	148	240	6.5	5.7	5.9	6.1
94	142	236	5.9	4.5	5.4	5.7
	144	238	6.5	5.3	6.1	5.9
	146	240	7.0	6.0	6.4	5.8
	148	242	7.1	6.4	6.3	5.7
	150	244	6.9	6.6	6.0	5.5
	152	246	7.2	6.3	5.7	5.4
96	146	242	7.1	6.6	6.7	6.0
	148	244	7.2	6.9	6.6	6.1
	150	246	6.8	7.0	6.2	6.0
	152	248	6.6	6.8	5.9	5.9
	154	250	5.9	5.9	5.3	5.4
98	152	250	6.5	7.1	6.5	5.6
	154	252	–	6.1	5.8	5.3

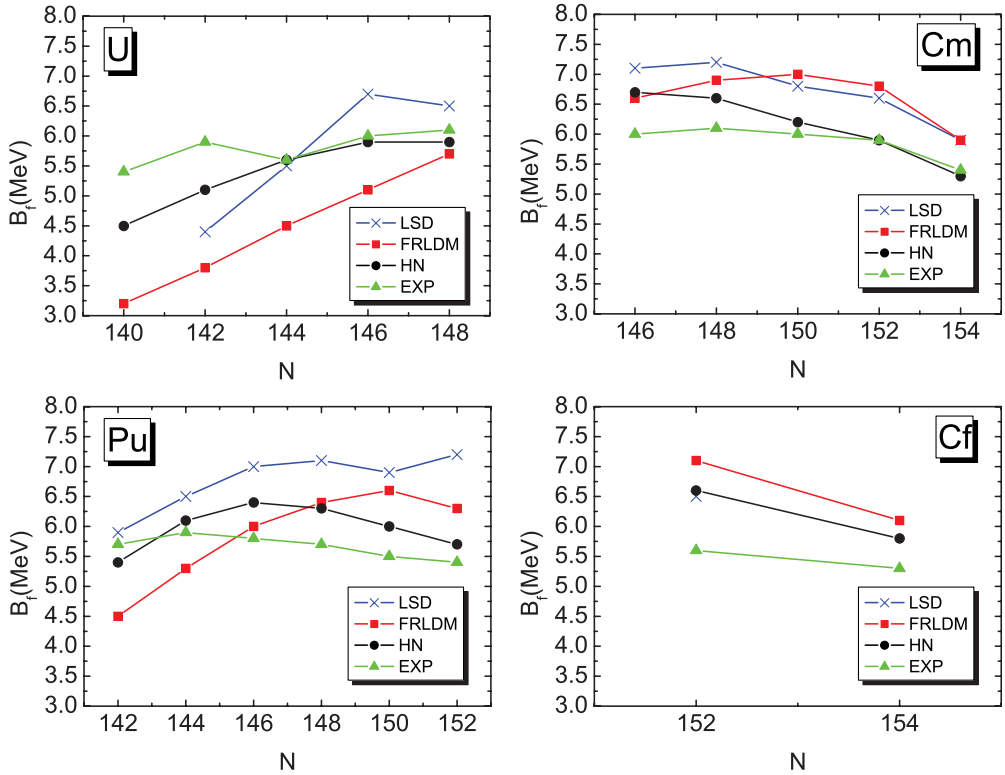

FIG. 1. (Color online) Comparison of the first fission barriers calculated by Dobrowolski *et al.* (LSD) (Ref. [47]), Möller *et al.* (FRLDM) (Ref. [19]), and by us (HN) with experimental data (EXP) (Refs. [34,48]) for nuclei with the atomic number $Z = 92$, 94, 96, and 98.

down to adding an appropriately chosen constant value at the ground state. In reality, a proper treatment of this energy along the fission path is quite a difficult problem, see [44]. The calculation presented here has been performed without adding any zero-point vibration energy. The obtained HN results are compared in Fig. 1 with calculations to be found in the literature and which are based on the finite range liquid drop model (FRLDM) by Möller *et al.* [19,45] (marked with filled squares), on the Lublin-Strasbourg liquid drop (LSD) model [46,47] (denoted by crosses), and on the available experimental (EXP) values [34,48] (shown by full triangles).

It is worth noting that all approaches discussed here are based on the macroscopic-microscopic method. The essential difference comes from the parametrization of the macroscopic energy. All models contain the possibility to describe nonaxial shapes. Important differences can, however, be observed in the shape parametrization of a fissioning nucleus, and thus in the deformation space used in the calculation. The shell correction energy and the residual pairing interaction are also taken into account in different ways in the different models.

It is rather difficult to draw unambiguous conclusions from the presented results for actinides. However, one can see that a larger disagreement with the various models is observed for the element uranium. The comparison of our results for Cm isotopes and those obtained from the FRLDM and LSD models shows that the latter predictions are systematically higher than ours. Our results for the plutonium isotopes ($Z = 94$) usually lie between the values obtained using the other models. All of the presented models give too high fission barrier heights for californium isotopes. Despite some discrepancies, the values of the inner fission barrier heights obtained here are similar to the experimental values. The difference between our theoretical calculations and experimental values [34,48] is shown in Fig. 2. The theoretical values of barrier heights are systematically higher than the experimental ones. They could be reduced further when taking into account the higher multipolarities in the radius expansion (i.e., choosing a richer deformation space).

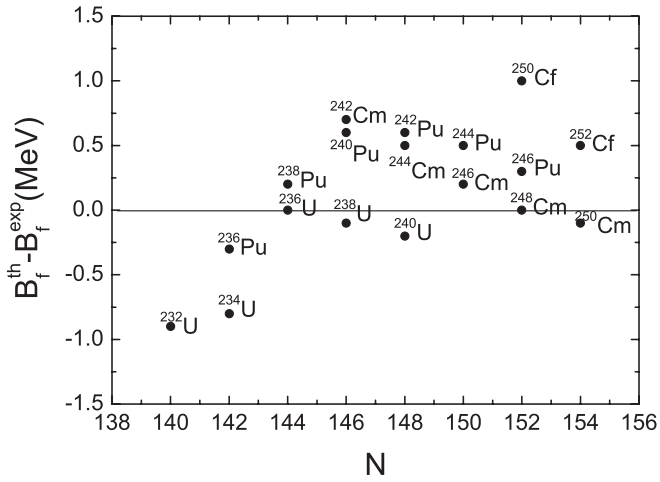

FIG. 2. Difference between theoretical and experimental [34,48] inner fission barrier heights for even-even actinide nuclei as a function of the neutron number.

TABLE II. Statistical parameters of calculated inner fission barrier heights in various macroscopic-microscopic models. All quantities are in MeV, except for the number of nuclei N.

Models	LSD	FRLDM	HN
N	16	18	18
$\langle\lvert B_f^{\rm th} - B_f^{\rm expt}\rvert\rangle$	0.9	1.0	0.4
$\mathrm{Max}\lvert B_f^{\rm th} - B_f^{\rm expt}\rvert$	1.8	2.2	1.0
rms	1.0	1.1	0.5

Table II contains some statistical parameters that describe the precision of the different calculations with respect to the experimental data for the different macroscopic-microscopic methods we discussed. The average discrepancy $\langle\lvert B_f^{\rm th} - B_f^{\rm expt}\rvert\rangle$, the maximal difference $\mathrm{Max}\lvert B_f^{\rm th} - B_f^{\rm expt}\rvert$, and the rms deviation are shown for a number N of even-even heavy nuclei.

We believe that these results are quite spectacular with an rms deviation from experimental results which is only half that of other models, and average and maximal differences which are much smaller. However, this is not very surprising if one takes into account that the presented model is specially adapted for the heaviest nuclei. A relatively small number of nuclei are considered here as compared to the global mass fits performed in the framework of FRLDM and LSD models where more than 2000 nuclei were considered.

Before continuing further, we would like to mention that, unfortunately, experimentally the fission barriers are accessible only indirectly and model-dependent analysis is involved to obtain these quantities, which causes a certain ambiguity in the comparison.

B. Potential-energy surface

It is commonly known that the action integral giving the tunneling probability depends strongly, among other things, on the potential barrier shapes, and even seemingly insignificant changes of this barrier can change the obtained half-lives by a few orders of magnitude. We therefore need to investigate very carefully the potential-energy surface obtained in the framework of our macroscopic-microscopic model in the multidimensional deformation space. The potential-energy surface calculated in the seven-dimensional space is projected in Fig. 3 on the (β_2, γ_2) plane, which means that it is shown as a function of β_2, γ_2, but at each given (β_2, γ_2) point it is minimized in the remaining degrees of freedom (denoted by the index m in the specification of the deformation parameters). This is shown in Fig. 3 for a very heavy compound system with neutron number $N = 182$ (close to the spherical magic neutron number $N = 184$) and proton number $Z = 120$ which, after the observation of element $Z = 118$ [2] and its confirmation, [6] is a natural candidate for further experimental studies. A first attempt to synthesize the element $Z = 120$ in a hot fusion reaction $^{58}\mathrm{Fe} + ^{244}\mathrm{Pu} \rightarrow ^{302-xn}120 + xn$ has already been undertaken by Oganessian *et al.* [4]. No decay chains were observed during an irradiation of a ^{244}Pu target with a beam of ^{58}Fe projectiles. Another possible entrance channel with a combination of well-deformed actinide targets and projectiles leading to this nucleus in a hot fusion reaction could be, among

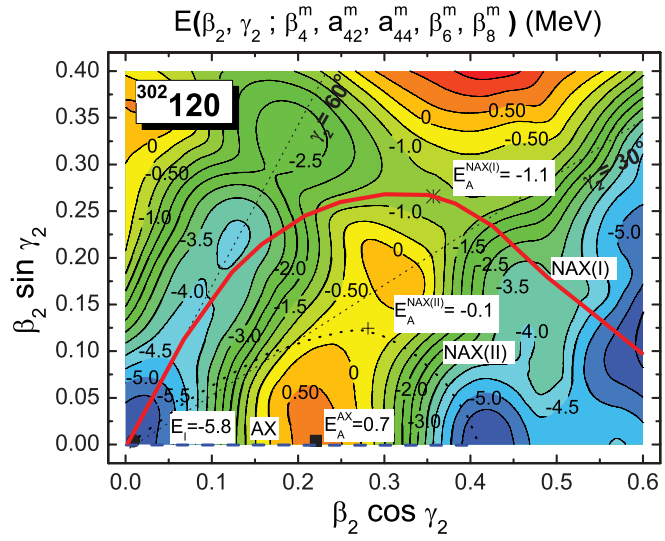

FIG. 3. (Color online) Contour map of the potential-energy surface of the nucleus $^{302}120$. Positions of the ground state [E_I (circle)] and higher [$E_A^{\rm NAX(II)}$ (cross)] and lower [$E_A^{\rm NAX(I)}$ (star)] nonaxial saddle points are indicated. The axial saddle point $E_A^{\rm AX}$ is marked by a filled square.

others: $^{64}\mathrm{Ni} + ^{238}\mathrm{U}$, $^{54}\mathrm{Cr} + ^{248}\mathrm{Cm}$, and $^{50}\mathrm{Ti} + ^{249}\mathrm{Cf}$ with the $3n$ and $4n$ neutron evaporation channels.

The energy is normalized in such a way that its macroscopic part is set equal to zero at the spherical shape of a nucleus. One can see that, as expected, the equilibrium point (ground state) is obtained at the spherical shape, while the saddle point is obtained at a nonaxial shape. The parameters of the shape are $\beta_2^{\rm sp} = 0.449$, $\gamma_2^{\rm sp} = 32.3^\circ$, $\beta_4^{\rm sp} = 0.020$, $a_{42}^{\rm sp} = -0.008$, $\beta_{44}^{\rm sp} = 0.004$, $\beta_6^{\rm sp} = 0.011$, $\beta_8^{\rm sp} = -0.015$. It is seen that the quadrupole deformation is the most important component. Its parameters are much larger than those of higher multipolarity. This finds a direct reflection in the contribution to energy of the nucleus at its saddle point. It is also interesting to notice that there appears a second saddle point with an energy $E_A^{\rm NAX(I)} = -0.1$ MeV, 1 MeV above the energy of the lower saddle $E_A^{\rm NAX(II)} = -1.1$ MeV and with a quite different shape, thus corresponding to a different structure of the nucleus. The rather small difference in energy at the two saddles allows one to speculate that in neighboring nuclei, the second saddle may be lower in energy than the first one, leading to large differences in the shape and structure, and, consequently, in the properties of the neighboring nuclei at their saddle points. As follows from the Introduction, the precise knowledge of the barrier shapes that depend on the deformation is necessary for the correct estimate of the tunneling probability. Figure 4 shows variation of the effective static fission path in the (β, γ) plane in the case of an axial path and of a nonaxial path. Note that the static paths in the full-dimensional deformation space are roughly 1.5 times longer than these projections. By analyzing the diagrams it can be seen that the position of the curve maximum (nonaxial saddle point, $E_A^{\rm NAX(I)}$) denoted by the solid line corresponds to the position of the exit point for the axial fission path (the curve is denoted by the broken line). It can lead to essential differences in the values of the

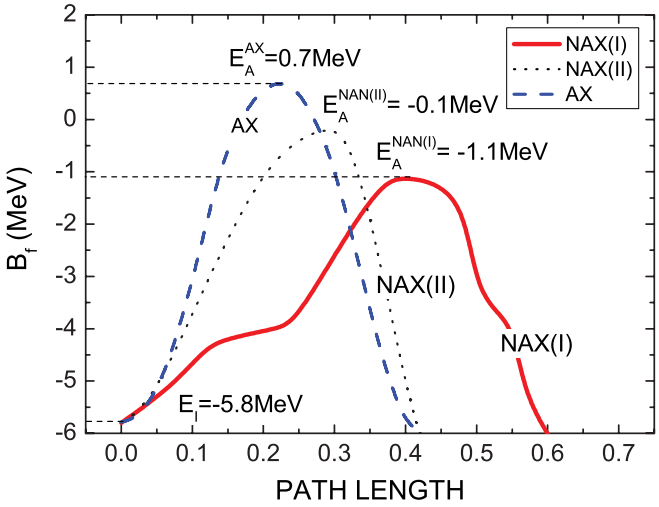

FIG. 4. (Color online) Axially symmetric (dashed) and nonaxial static fission barriers in the $^{302}120$ vs Euclidean length of the path in the (β, γ) plane.

action integral, tunneling probabilities, and consequently in the calculated half-lives.

C. Importance of nonaxiality

The role of triaxiality on static fission barriers has been shown before in many publications (see, e.g., [31,32,47,49–53]) and recently in our paper [54]. The main conclusion which can be drawn from this study is that the largest reduction of the barrier height due to the quadrupole (γ_2) nonaxial deformation is about 2 MeV and appears in two regions of the nuclei: one for $Z \approx 100$ and $N \approx 158$ and the other with $Z \approx 122$ and $N \approx 180$.

Let us now investigate the importance of hexadecapole nonaxial deformations. As was mentioned in the preceding section, it has been always assumed so far that the hexadecapole axial asymmetry parameters are either zero or directly related to the quadrupole deformation γ_2. One finds that a more accurate inclusion of these hexadecapole nonaxiality deformation parameters can lead to a reduction of the fission barriers by up to about 1.5 MeV in the vicinity of $Z \approx 122$ and $N \approx 160$.

However, one can notice that the effect appears only in a few nuclei of a rather small part of the investigated region. Details of the studies of the above effect can be found in our previous paper [55]. We have also checked whether the nonaxial effect that comes from higher multipolarities like β_{62}, β_{64}, β_{66} is of any importance for the barrier heights. Results obtained for all nuclei investigated in the present paper indicate that the largest effect of β_6-nonaxial shapes occurs only for several nuclei and is smaller than 300 KeV (i.e., comparable with the level of the used method errors). Therefore, we will neglect nonaxiality connected with β_6 in the further analysis. Some discussion of the effect of the multipolarity six nonaxial deformations on the saddle-point energy has been presented in Ref. [56]. Furthermore, in the case of heavy and superheavy nuclei, odd mulipolarities show up at rather large quadrupole deformations so that their influence on the first (A) maximum in the actinides, and on the first (A) and second (B) peak in superheavy nuclei is practically negligible.

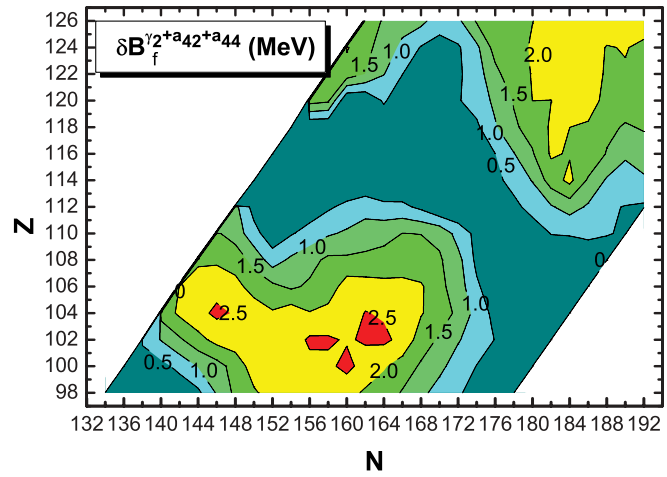

FIG. 5. (Color online) Contour map of the effect of fully incorporated nonaxiality deformations (γ_2, a_{42}, a_{44}) on the fission barrier heights B_f.

The main goal of our present analysis is to determine the influence of fully incorporated nonaxiality γ_2, a_{42}, a_{44} deformation, all together, on the fission barrier heights. Figure 5 illustrates the mentioned effect of the investigated nuclei.

One can see that the effect of nonaxialty reduces fission barrier heights by about 2.5 MeV for two regions of nuclei: one rather large region located around $100 \leqslant Z \leqslant 104$ and $156 \leqslant N \leqslant 164$ and a second region, which lies close to the nucleus with $Z \approx 104$ and $N \approx 146$.

D. Fission barriers for superheavy nuclei

In Fig. 6 we display the height of the fission barriers B_f (tabulated in Table III) for these nuclei calculated within the macroscopic-microscopic model as the difference between the total ground state E_I and the highest saddle-point energy $E_{A(B)}$. The figure contains the fission barriers heights $B_f = E_{A(B)} - E_I$ for superheavy elements in the range of proton number $98 \leqslant Z \leqslant 126$ and neutron number $134 \leqslant N \leqslant 192$.

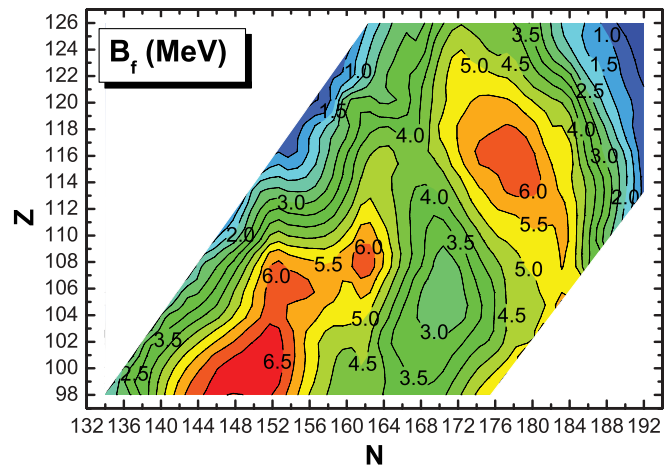

FIG. 6. (Color online) Contour map of calculated fission barrier heights B_f for even-even superheavy nuclei.

TABLE III. Calculated fission barrier heights (in MeV).

N	A	B_f	N	A	B_f	N	A	B_f	N	A	B_f	N	A	B_f
	$Z = 98$			$Z = 100$			$Z = 102$			$Z = 104$			$Z = 106$	
134	232	2.24	136	236	2.56	138	240	2.75	140	244	2.56	142	248	2.21
136	234	2.73	138	238	3.54	140	242	3.55	142	246	3.29	144	250	2.85
138	236	3.63	140	240	4.41	142	244	4.32	144	248	3.82	146	252	3.59
140	238	4.81	142	242	5.24	144	246	4.95	146	250	4.34	148	254	4.50
142	240	5.79	144	244	5.91	146	248	5.54	148	252	5.06	150	256	5.46
144	242	6.43	146	246	6.49	148	250	6.05	150	254	5.74	152	258	6.22
146	244	6.51	148	248	6.71	150	252	6.52	152	256	6.36	154	260	6.28
148	246	6.48	150	250	6.83	152	254	6.76	154	258	5.87	156	262	6.05
150	248	6.56	152	252	6.85	154	256	6.15	156	260	5.72	158	264	5.88
152	250	6.50	154	254	6.11	156	258	5.27	158	262	5.28	160	266	5.37
154	252	5.79	156	256	5.29	158	260	4.80	160	264	5.21	162	268	5.71
156	254	4.97	158	258	4.66	160	262	4.64	162	266	5.05	164	270	4.82
158	256	4.47	160	260	4.14	162	264	4.64	164	268	4.25	166	272	3.88
160	258	4.16	162	262	4.49	164	266	3.75	166	270	3.40	168	274	3.02
162	260	4.41	164	264	4.01	166	268	3.20	168	272	2.91	170	276	2.78
164	262	3.97	166	266	3.53	168	270	3.13	170	274	2.63	172	278	2.84
166	264	3.65	168	268	3.33	170	272	3.04	172	276	2.79	174	280	3.46
168	266	3.56	170	270	3.39	172	274	3.36	174	278	3.33	176	282	4.04
170	268	3.82	172	272	3.90	174	276	3.82	176	280	4.04	178	284	4.77
172	270	4.41	174	274	4.46	176	278	4.18	178	282	4.72	180	286	4.90
174	272	5.06	176	276	4.92	178	280	4.84	180	284	4.83	182	288	5.19
176	274	5.61	178	278	5.44	180	282	5.01	182	286	5.14	184	290	5.35
178	276	6.10	180	280	5.69	182	284	5.25	184	288	5.32	186	292	4.11
	$Z = 108$			$Z = 110$			$Z = 112$			$Z = 114$			$Z = 116$	
144	252	2.09	146	256	1.38	148	260	1.24	150	264	1.78	152	268	1.05
146	254	2.82	148	258	2.21	150	262	2.64	152	266	2.25	154	270	0.96
148	256	3.67	150	260	3.40	152	264	3.47	154	268	2.08	156	272	1.60
150	258	4.82	152	262	4.61	154	266	3.31	156	270	2.24	158	274	2.52
152	260	6.00	154	264	4.46	156	268	3.24	158	272	2.91	160	276	3.50
154	262	5.76	156	266	4.37	158	270	3.60	160	274	3.80	162	278	4.39
156	264	5.59	158	268	4.54	160	272	4.35	162	276	4.69	164	280	4.67
158	266	5.47	160	270	5.09	162	274	5.17	164	278	4.64	166	282	4.43
160	268	5.87	162	272	5.83	164	276	4.81	166	280	4.26	168	284	4.41
162	270	6.42	164	274	5.19	166	278	4.29	168	282	4.03	170	286	4.67
164	272	5.49	166	276	4.32	168	280	3.64	170	284	4.22	172	288	5.42
166	274	4.37	168	278	3.64	170	282	3.69	172	286	4.82	174	290	6.03
168	276	3.56	170	280	3.13	172	284	4.29	174	288	5.53	176	292	6.22
170	278	2.87	172	282	3.61	174	286	5.01	176	290	5.83	178	294	6.28
172	280	3.04	174	284	4.35	176	288	5.48	178	292	6.34	180	296	6.07
174	282	3.82	176	286	4.96	178	290	5.61	180	294	6.27	182	298	5.43
176	284	4.41	178	288	5.20	180	292	5.70	182	296	5.66	184	300	5.20
178	286	4.84	180	290	5.43	182	294	5.69	184	298	5.08	186	302	3.83
180	288	5.13	182	292	5.38	184	296	5.41	186	300	4.35	188	304	2.87
182	290	5.23	184	294	5.50	186	298	4.33	188	302	3.33	190	306	1.97
184	292	5.43	186	296	4.11	188	300	3.25	190	304	2.11	192	308	0.59
186	294	4.07	188	298	2.73	190	302	1.91	192	306	0.81			
188	296	2.83	190	300	1.52	192	304	0.75						

TABLE III. (*Continued.*)

N	A	B_f	N	A	B_f	N	A	B_f	N	A	B_f	N	A	B_f
	$Z = 118$			$Z = 120$			$Z = 122$			$Z = 124$			$Z = 126$	
154	272	0.59	156	276	0.41	158	280	0.80	160	284	0.86	162	288	1.39
156	274	1.36	158	278	0.86	160	282	1.22	162	286	1.81	164	290	2.16
158	276	2.17	160	280	2.92	162	284	2.10	164	288	2.60	166	292	2.85
160	278	2.91	162	282	3.26	164	286	2.92	166	290	3.09	168	294	2.88
162	280	3.78	164	284	2.94	166	288	3.32	168	292	3.28	170	296	3.82
164	282	4.09	166	286	3.16	168	290	3.84	170	294	4.41	172	298	4.43
166	284	3.88	168	288	4.02	170	292	4.72	172	296	4.99	174	300	4.31
168	286	4.05	170	290	4.80	172	294	5.32	174	298	4.71	176	302	4.08
170	288	5.06	172	292	5.33	174	296	5.25	176	300	4.40	178	304	4.01
172	290	5.54	174	294	5.56	176	298	5.03	178	302	4.36	180	306	3.38
174	292	5.86	176	296	5.64	178	300	4.84	180	304	3.72	182	308	2.48
176	294	5.99	178	298	5.50	180	302	4.23	182	306	2.79	184	310	1.70
178	296	6.04	180	300	5.05	182	304	3.74	184	308	2.07	186	312	1.43
180	298	5.72	182	302	4.66	184	306	3.13	186	310	1.43	188	314	0.81
182	300	5.08	184	304	4.20	186	308	1.96	188	312	1.24	190	316	0.29
184	302	4.82	186	306	2.87	188	310	1.42	190	314	0.68	192	318	0.00
186	304	3.51	188	308	1.77	190	312	0.90	192	316	0.14			
188	306	2.43	190	310	1.17	192	314	0.36						
190	308	1.37	192	312	0.75									
192	310	0.56												

It can be seen that in the whole region of considered nuclei the barriers are smaller than 7 MeV. The highest values are obtained for the nuclei $^{270}108_{162}$, $^{292}114_{178}$, and around the nucleus $Z \approx 100$, $N \approx 150$.

Another important observation concerns the behavior of fission barrier heights with increasing proton number of these heaviest nuclei. One can recognize that the quite high barrier for $^{296}118_{178}$ rapidly decreases, reaching a value 1.43 MeV for the $^{312}126_{186}$ nucleus. Obviously such a compound system does not have any chance to survive against fission in our model. This is in a contradiction to self-consistent models, according to which the fission barrier for a neighboring nucleus is about 12 MeV [57]!

Next we turn to the discussion of whether or not the obtained values can be useful for future experiments. In Table IV we collect some of the theoretical prediction of fission barrier heights based on the FRLDM [19], the self-consistent Hartree-Fock (SHF) method [58] with the SLy6 Skyrme interaction [59], the extended Thomas-Fermi plus Strutinsky integral (ETFSI) model [60] in relation to experimental ones [61] and our predictions (HN). Note that lower limits for the fission barrier heights are evaluated in Ref. [61]. As we can see, experimental and calculated barrier heights are in agreement while both FRLDM and SHF significantly overestimate the barrier. This behavior concerning fission barriers is well known from earlier calculations in self-consistent models [57]. Surprisingly the modern version of the microscopic-macroscopic calculation presented in Ref. [19] (including nonaxial shapes) gives values comparable to the axially symmetrical calculations of SHF and overestimates the experimental barriers in a similar way. This tendency is also visible, to a lesser extent, for heavier systems. Thus for the element $^{292}116_{176}$ the FRLDM model gives a value of 9.26 MeV for the barrier height while the value obtained in our approach (6.22 MeV) is about 3 MeV lower, whereas the experimental data indicate 6.4 MeV. For the neighboring isotope $^{292}116_{178}$ the experimentally predicted fission barrier is also 6.4 MeV and we obtain almost the same value 6.28 MeV, but estimations based on the FRLDM predict a value of 9.46 MeV, almost 3 MeV larger. As a consequence, such high barriers result in cross

TABLE IV. Comparison of fission barrier heights (in MeV) with other theoretical evaluations: SHF [58], FRLDM [19], ETFSI [60], HN (present paper), and experimental data taken from Ref. [61].

Nucleus	SHF	FRLDM	ETFSI	HN	EXP
$^{284}112_{172}$	6.06	7.41	2.2	4.29	5.5
$^{286}112_{174}$	6.91	8.24	3.6	5.01	5.5
$^{288}114_{174}$	8.12	9.18	6.1	5.53	6.7
$^{290}114_{176}$	8.52	9.89	6.6	5.83	6.7
$^{292}114_{178}$	–	9.98	7.2	6.34	6.7
$^{292}116_{176}$	9.35	9.26	6.5	6.22	6.4
$^{294}116_{178}$	9.59	9.46	7.2	6.28	6.4
$^{296}116_{180}$	–	9.10	7.2	6.07	6.4
$^{294}118_{176}$	–	8.48	6.6	5.99	–
$^{296}118_{178}$	–	8.36	7.0	6.04	–
$^{298}118_{180}$	–	8.05	7.4	5.72	–
$^{296}120_{176}$	–	7.69	6.2	5.64	–
$^{298}120_{178}$	–	7.33	6.6	5.50	–
$^{300}120_{180}$	–	7.01	6.8	5.05	–
$^{302}120_{182}$	–	6.07	7.2	4.66	–
$^{304}120_{184}$	–	4.86	6.8	4.20	–

sections for $Z = 114, 116, 118$, and 120 which overestimate the experimental data by several orders of magnitude [62,63]. The ETFSI model significantly underestimates the barrier heights for $^{284}112_{172}$, and $^{286}112_{174}$. For heavier systems the agreement is, however, much better. One must keep in mind that SHF models include neither quadrupole nor higher nonaxial degrees of freedom and the observed discrepancies probably can be explained by the absence of these variables at the saddle-point configuration.

V. CONCLUSIONS

One of the most important ingredients used to calculate the survival probability of superheavy elements synthesized in heavy-ion reactions is the fission barrier height B_f, which allows us to estimate the competition between the fission process and particle emission. The following conclusions can be drawn from our investigation that was devoted to these quantities in heavy and superheavy elements.

(i) The above presented model which contains no adjustable parameters has been applied to 18 even-even elements with $Z \geqslant 92$, where the first fission barriers are experimentally known. The largest discrepancy with the experimental data is only about 1.0 MeV (i.e., of the order of magnitude of the discrepancy between various experimental data), while the average discrepancy is about 0.4 MeV and the root-mean-square deviation has a value 0.5 MeV.

(ii) Taking into account triaxial deformations has been shown to significantly reduce the fission barrier heights by up to 2.5 MeV.

(iii) It has been demonstrated that the inclusion of higher multipolarities can lead to a significant change of the fission path in the multidimensional deformation space and can consequently cause a considerable change of the fission half-lives.

(iv) Our calculations indicate that, in contrast to self-consistent mean-field calculations of fission barriers, the barrier height, which is still quite substantial for a nuclei with $Z = 118$ becomes lower than 4.5 MeV for nuclei with $Z = 126$.

(v) Theoretical evaluations of fission barrier heights based on various models differ between each other significantly. It is obvious that future experiments on superheavy nuclei will constitute a natural benchmark for all theoretical models describing these nuclei.

In the forthcoming paper we are going to extend our study on odd nuclei. A systematic determination of the half-lives for heavy and superheavy elements is under construction as well.

ACKNOWLEDGMENTS

We would like to thank Sigurd Hofmann and all of the members of the SHIP group for fruitful discussions and for the warm hospitality extended to us during our stay in the GSI laboratory, where a large part of the present work was completed. We gratefully acknowledge stimulating and enlightening discussion with Peter Möller, Zygmunt Patyk, Krzysztof Pomorski, Piotr Rozmej, and Janusz Skalski. We express our gratitude to Johny Bartel for many valuable suggestions and a careful reading of the manuscript. Support by the Polish Ministry of Science and Higher Education, Grant No. 1-P03B-042-30, by Helmholtzinstitute Mainz (HIM), as well as Polish-JINR (Dubna) Cooperation Programme, is gratefully acknowledged.

APPENDIX: SADDLE-POINT SEARCHING TECHNIQUE

It is always possible to convert the m-dimensional grid: $(n_1 \times n_2 \times n_3 \times \cdots \times n_m)$ into a four-dimensional grid: $(n_1 \times n_2 \times n_3 \times N)$, $N = n_4 \times n_5 \times n_6 \times \cdots \times n_m$. In the case of our deformation space: $n_1 = \beta_2$ (elongation), $n_2 = \gamma_2$ (nonaxility), $n_3 = \beta_4$ (neck). The N axis describes all other degrees of freedom which we use for the description of shapes (all other multipolarities). Each path i, connecting the starting point and $n + 1$ point, may be characterized by the maximal value of energy $E^i_{\max}$ which one can find along it, where i is the index of a given path. The values of the energy between two neighboring points on a given path are also investigated with the help of an interpolation procedure. In this way, we have a set of all possible paths i from the starting point to the $n + 1$ point with the value of maximal energy $E^i_{\max}$ on each path. It is obvious that the value of the energy in the saddle point will be the minimal value of all the $E^i_{\max}$ obtained along all possible paths (all possible i). The trajectory, corresponding to this minimal value, will automatically pass through the saddle point. It appears that to find the right trajectory along which $E^i_{\max}$ is minimal, we do not need to consider all possible trajectories. This method, which allows us to restrict the number of considered paths to a very small number, as compared to all possible trajectories, is called the "*dynamic programming method*" [30].

[1] Yu. Ts. Oganessian *et al.*, Phys. Rev. Lett. **83**, 3154 (1999); Nature (London) **400**, 242 (1999); Phys. Rev. C **62**, 041604 (2000); **63**, 011301(R) (2000); **69**, 054607 (2004).
[2] Yu. Ts. Oganessian *et al.*, Phys. Rev. C **74**, 044602 (2006).
[3] Yu. Ts. Oganessian *et al.*, Phys. Rev. Lett. **104**, 142502 (2010).
[4] Yu. Ts. Oganessian *et al.*, Phys. Rev. C **79**, 024603 (2009).
[5] TASCA report, GSI Kurier 31 (2009) (unpublished).
[6] L. Stavsetra *et al.*, Phys. Rev. Lett. **103**, 132502 (2009).
[7] G. G. Adamian, N. V. Antonenko, and W. Scheid, Phys. Rev. C **69**, 044601 (2004).
[8] K. Siwek-Wilczyńska, I. Skwira, and J. Wilczyński, Phys. Rev. C **72**, 034605 (2005).
[9] A. Baran, Z. Łojewski, K. Sieja, and M. Kowal, Phys. Rev. C **72**, 044310 (2005).
[10] W. Loveland, Phys. Rev. C **75**, 069801 (2007).
[11] Y. Aritomo, Phys. Rev. C **75**, 024602 (2007).
[12] Z. H. Liu and Jing-Dong Bao, Phys. Rev. C **76**, 034604 (2007).
[13] V. Zagrebaev and W. Greiner, Phys. Rev. C **78**, 034610 (2008).

[14] J. C. Pei, W. Nazarewicz, J. A. Sheikh, and A. K. Kerman, Phys. Rev. Lett. **102**, 192501 (2009).
[15] Zhao-Qing Feng, Gen-Ming Jin, and Jun-Qing Li, Phys. Rev. C **76**, 044606 (2007).
[16] Z. H. Liu and Jing-Dong Bao, Phys. Rev. C **80**, 054608 (2009).
[17] S. K. Patra, R. N. Panda, P. Arumugam, and Raj K. Gupta, Phys. Rev. C **80**, 064602 (2009).
[18] A. Sobiczewski and M. Kowal, Int. J. Mod. Phys. E **18**(4), 869 (2009).
[19] P. Möller *et al.*, Phys. Rev. C **79**, 064304 (2009).
[20] I. Muntian, Z. Patyk, and A. Sobiczewski, Acta Phys. Pol. B **32**, 691 (2001).
[21] I. Muntian, Z. Patyk, and A. Sobiczewski, Yad. Fiz. **66**, 1051 (2003).
[22] H. J. Krappe, J. R. Nix, and A. J. Sierk, Phys. Rev. C **20**, 992 (1979).
[23] V. M. Strutinski, Sov. J. Nucl. Phys. **3**, 449 (1966); Nucl. Phys. A **95**, 420 (1967).
[24] S. Ćwiok, J.-Dudek, W. Nazarewicz, J. Skalski, and T. Werner, Comput. Phys. Commun. **46**, 379 (1987).
[25] H. Hofmann, *The Physics of Warm Nuclei* (Oxford University Press, New York, 2008).
[26] R. W. Hasse and W. D. Myers, *Geometrical Relationships of Macroscopic Nucler Physics* (Springer-Verlag, Berlin, 1988).
[27] P. Möller, R. Bengtsson, B. G. Carlsson, P. Olivius, and T. Ichikawa, Phys. Rev. Lett. **97**, 162502 (2006).
[28] P. Jachimowicz, M. Kowal, P. Rozmej, J. Skalski, and A. Sobiczewski, Int. J. Mod. Phys. E **18**(4), 1088 (2009); **19**(4), 768 (2010).
[29] P. Jachimowicz, M. Kowal, and J. Skalski, Int. J. Mod. Phys. E **19**(4), 508 (2010).
[30] A. Baran, K. Pomorski, A. Łukasiak, and A. Sobiczewski, Nucl. Phys. A **361**, 83 (1981).
[31] S. Ćwiok and A. Sobiczewski, Z. Phys. A **342**, 203 (1992).
[32] R. A. Gherghescu, J. Skalski, Z. Patyk, and A. Sobiczewski, Nucl. Phys. A **651**, 237 (1999).
[33] V. Luc and P. Soille, IEEE Trans. Pattern Anal. Mach. Intell. **13**, 583 (1991).
[34] A. Mamdouh, J. M. Pearson, M. Rayet, and F. Tondeur, Nucl. Phys. A **644**, 389 (1998).
[35] B. Hayes, Am. Sci. **88**, 481 (2000).
[36] P. Möller, A. J. Sierk, and A. Iwamoto, Phys. Rev. Lett. **92**, 072501 (2004).
[37] P. Möller, Nucl. Phys. A **192**, 529 (1972).
[38] R. Bengtsson *et al.*, Nucl. Phys. A **473**, 77 (1987).
[39] S. Ćwiok *et al.*, Phys. Lett. B **322**, 304 (1994).
[40] B. B. Back *et al.*, Phys. Rev. Lett. **28**, 1707 (1972).
[41] B. S. Bhandari and A. S. Al Kharam, Phys. Rev. C **39**, 917 (1989).
[42] F. M. Naumann *et al.*, Nucl. Phys. A **502**, 271 (1989).
[43] L. Csige *et al.*, Phys. Rev. C **80**, 011301(R) (2009).
[44] K. Pomorski, Int. J. Mod. Phys. E **17**(1), 245 (2008).
[45] P. Möller and J. R. Nix, At. Data Nucl. Data Tables **39**, 213 (1988); P. Möller *et al.*, *ibid*. **39**, 225 (1988).
[46] K. Pomorski and J. Dudek, Phys. Rev. C **67**, 044316 (2003).
[47] A. Dobrowolski, K. Pomorski, and J. Bartel, Phys. Rev. C **75**, 024613 (2007).
[48] G. N. Smirenkin, IAEA Report No. INDC(CCP)-359, Vienna, 1993.
[49] J. Dechargé, J. F. Berger, M. Girod, and K. Dietrich, Nucl. Phys. A **716**, 55 (2003).
[50] S. Ćwiok, J. Dobaczewski, P.-H. Heenen, P. Magierski, and W. Nazarewicz, Nucl. Phys. A **611**, 211 (1996).
[51] A. K. Dutta, J. M. Pearson, and F. Tondeur, Phys. Rev. C **61**, 054303 (2000).
[52] L. Bonneau, P. Quentin, and D. Samsoen, Eur. Phys. J. A **21**, 391 (2004).
[53] S. Ćwiok, P.-H. Heenen, and W. Nazarewicz, Nature (London) **433**, 709 (2005).
[54] M. Kowal and A. Sobiczewski, Int. J. Mod. Phys. E **18**(4), 914 (2009).
[55] A. Sobiczewski, P. Jachimowicz, and M. Kowal, Int. J. Mod. Phys. E **19**(4), 493 (2010).
[56] L. Shvedow, S. G. Rohoziński, M. Kowal, S. Belchikov, and A. Sobiczewski, Int. J. Mod. Phys. E **17**(1), 265 (2008).
[57] A. Staszczak, J. Dobaczewski, and W. Nazarewicz, Int. J. Mod. Phys. E **14**(3), 395 (2005); **16**(2), 310 (2007).
[58] T. Bürvenich, M. Bender, J. A. Maruhn, and P.-G. Reinhard, Phys. Rev. C **69**, 014307 (2004).
[59] E. Chabanat, P. Bonche, P. Haensel, J. Meyer, and R. Schaefer, Nucl. Phys. A **635**, 231 (1998); **643**, 441(E) (1998).
[60] A. Mamdouh, J. M. Pearson, M. Rayet, and F. Tondeur, Nucl. Phys. A **679**, 337 (2001).
[61] M. G. Itkis, Yu. Ts. Oganessian, and V. I. Zagrebaev, Phys. Rev. C **65**, 044602 (2002).
[62] K. Siwek-Wilczyńska, A. Borowiec, and J. Wilczyński, Int. J. Mod. Phys. E **18**(4), 1079 (2009).
[63] K. Siwek-Wilczyńska, T. Cap, and J. Wilczyński, Int. J. Mod. Phys. E **19**(4), 500 (2010).